Energy-Efficient RIS-assisted SWIPT System With Electromagnetic-Compliant Model

Jie Tang
School of Electronic and Information Engineering
South China University of Technology
Guangzhou, China
eejtang@scut.edu.cn

Ruoyan Ma*
School of Electronic and Information Engineering
South China University of Technology
Guangzhou, China
eeruoyan_ma@mail.scut.edu.cn

Xiu Yin Zhang
School of Electronic and Information Engineering
South China University of Technology
Guangzhou, China
eexyz@scut.edu.cn

Kai-Kit Wong
Department of Electronic and Electrical Engineering
University College London
London, U.K
kai-kit.wong@ucl.ac.uk

***Abstract*—In this article, we conduct the system optimization for a reconfigurable intelligent surface (RIS)-assisted simultaneous wireless power transfer (SWIPT) network. In particular, a problem of energy efficiency maximization subject to the physical limitations and quality of service (QoS) is introduced. Specifically, the existence of potential eavesdroppers and the physical features, which are exposed by the end-to-end transfer model based on the S-parameter analysis, of the main ends are considered. For tackling the above complicated issue, the Sherman-Morrison formula is first adopted to transform it into a more solvable form. Then the alternative solving approaches are introduced to optimize the beamforming vector of the transmitter, artificial noise, power splitting ratio of the dual-demand receiver, and reflection coefficient of the RIS iteratively. The results demonstrate the effectiveness of the proposed algorithms and the practice-oriented model.**

Keywords- SWIPT; RIS; S-parameter; Physical Model.

I. INTRODUCTION

The simultaneous wireless information and power transfer (SWIPT) system can meet the communication and power-supply requirements of sensor terminals with the same transceiver architecture [1-3]. In typical applied scenarios, terminal devices can continuously harvest energy from ambient electromagnetic sources, facilitated by the ever-present wireless signals [4]. In terms of system architecture, the receiving subsystem of SWIPT can be categorized into dual-demand and single-demand types. The dual-demand one entails simultaneous fulfillment of information demodulation (ID) and energy harvesting (EH), while single-demand requires satisfying only one of these tasks [5]. These architectures cater to different application scenarios, yet they both face challenges in ensuring reliable services due to sensitivity to transmission blockages.

Introducing reconfigurable intelligent surfaces (RIS) can effectively address the reliability issue in SWIPT transmission. Particularly, RIS enhances stability by reconstructing obstructed channels through its controllability [6, 7]. It achieves this by configuring its controller to adjust the elements in the array. Specifically, RIS allows incident waves to be reflected in desired directions. The regulation of reflected waves can be discrete or continuous, depending on the usage of positive-intrinsic-negative (PIN) diodes or varactors [8, 9]. RIS operates with very low energy consumption, making it an energy-efficient solution [10]. Its effectiveness extends to secure networks, further highlighting its promising performance [11].

While significant research focuses on RIS-aided SWIPT systems, few studies delve into the physical characteristics of RIS, which is crucial due to its electromagnetic nature. Incorporating electromagnetic analysis enhances relevance to real-world scenarios [12]. Various studies aim to construct practical RIS models, using circuit-based analysis to reveal the inductance, capacitance, and resistance of RIS components, yielding expressions for amplitude and phase shift [13]. Integrating radar theory portrays RIS as an anomalous reflection device, linking phase shift to electromagnetic field calculations, and exposing EM information of incident and reflection waves [14]. Additionally, the analysis approach of S-parameter is adopted for modeling and the channel is considered as an N-port network [15].

Inspired by prior studies, this paper investigates a MISO-downlink RIS-assisted SWIPT system, while also addressing the potential threat of information leakage for communication security. Specifically, this work utilizes the S-parameter, which is better suited for analyzing the scattering properties of RIS, to construct the communication model. For solving the proposed system problem. The coupled multiple variables are separated by the alternative solution. Particularly, the successive convex approximation (SCA) and Sherman-Morrison formula based approaches are introduced to resolve the subproblems.

II. SYSTEM MODEL AND PROBLEM FORMULATION

With analysis approaches of S-parameter, we can achieve the end-to-end electromagnetic model as (1), where $\mathbf{Q} = \mathbf{\Gamma}_R + \mathbf{I}$. Its specific analysis process can be found in [16] and we don't present more details here. Moreover, $\mathbf{\Gamma}_R$ denotes the reflection coefficient matrix of the transmitter. The matrices, which has t-

This work is supported by the National Natural Science Foundation of China under Grant 62222105. The marker "*" denotes the corresponding author.

$$\mathbf{H}_{E2E}(\boldsymbol{\Theta}) = \mathbf{Q}(\mathbf{I}-\mathbf{S}_{RR}\boldsymbol{\Gamma}_R)^{-1}\mathbf{S}_{RT}(\mathbf{I}+\mathbf{S}_{TT})^{-1} + \mathbf{Q}(\mathbf{I}-\mathbf{S}_{RR}\boldsymbol{\Gamma}_R)^{-1}\mathbf{S}_{RI}(\boldsymbol{\Theta}^{-1}-\mathbf{S}_{II})^{-1}\mathbf{S}_{IT}(\mathbf{I}+\mathbf{S}_{TT})^{-1}. \quad (1)$$

he form of $\mathbf{S}_{AB}$, are the self-S-parameter parameters of the different ends (transmitter, receiver, and RIS). What's more, the matrices with the form $\mathbf{S}_{AB}$ are the transmission parameters between the two ends. It is worth mentioning that the S-parameter-based model can reveal a lot of crucial features of the communication systems. Theoretically, all electromagnetic devices can be inserted into the model for expansion.

(1) has the multiple-input multiple-output (MIMO) form, which is a general expression. When we omit the physical features of the transmitter and the receiver and simplify the model to the multiple-input single-output (MISO) form, the model can be written as

$$\mathbf{h}(\boldsymbol{\Theta}) = \mathbf{s}_{RT} + \mathbf{s}_{RI}(\boldsymbol{\Theta}^{-1}-\mathbf{S}_{II})^{-1}\mathbf{S}_{IT}. \quad (2)$$

With (2), we can describe the RIS-assisted SWIPT network with two types of receivers (dual-demand one and single-demand one) as in Fig. 1. The dual-demand type uses the power-splitting approach to separate the energy and information streams. We then give the received signal for the demodulation of the dual-demand user as

$$y_n = \sqrt{\rho_n}\left(\mathbf{h}_n\left(\sum_{n=1}^{N_D}\mathbf{w}_n s_n + \mathbf{z}\right) + n_1\right) + n_2, \quad (3)$$

where ρ_n is the power-splitting ratio, $\mathbf{w}_n$ is the beamforming vector, $\mathbf{z}$ is the artificial noise for interrupting the illegal demodulation of single-demand users with only energy demand. n_1 is the noise at the antenna with the power σ_1^2 and n_2 is the noise during the demodulation with the power δ_2^2. Relying on (3), the signal-to-interference plus noise ratio (SINR) and harvested radio-frequency (RF) power of the n^{th} dual-demand users are

$$\gamma_n = \frac{|\mathbf{h}_n\mathbf{w}_n|^2}{|\mathbf{h}_n\mathbf{z}|^2 + \sum_{k\neq n}^{N_D}|\mathbf{h}_n\mathbf{w}_k|^2 + \sigma_1^2 + \frac{\delta_2^2}{\rho_n}}, \quad (4)$$

$$P_{\mathrm{EH},n} = (1-\rho_n)\left(\mathbf{h}_n\left(\sum_{n=1}^{N_D}\mathbf{w}_n\mathbf{w}_n^H + \mathbf{Z}\right)\mathbf{h}_n^H\right), \quad (5)$$

Similarly, the harvested power of single-demand user can also follow (5). However, when the l^{th} single-demand user tries to demodulate the information of the n^{th} DDR, the SINR of the information leakage can be rewritten as

$$\gamma_{l,n} = \frac{|\mathbf{h}_l\mathbf{w}_n|^2}{|\mathbf{h}_l\mathbf{z}|^2 + \sum_{k\neq n}^{N_D}|\mathbf{h}_l\mathbf{w}_k|^2 + \sigma_1^2 + \delta_2^2}. \quad (6)$$

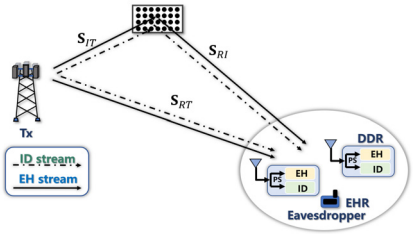

Figure 1. The scenario for RIS-assisted SWIPT

With the above analysis, the system problem can be formulated to satisfy the basic requirements of the users and restrict the potential information leakage.

$$\mathbf{P}_0: \quad \max \frac{\sum_{n=1}^{N_D} R_n(\mathbf{w}_n, \rho_n, \boldsymbol{\Theta}, \mathbf{z})}{P_{\mathrm{total}}(\mathbf{w}_n, \rho_n, \boldsymbol{\Theta}, \mathbf{z})} \quad (7a)$$

$$\text{s.t. } P_T \le P_{\mathrm{Max}}, \quad (7b)$$

$$\gamma_n(\mathbf{w}_n, \rho_n, \boldsymbol{\Theta}, \mathbf{z}) \ge 2^{R_n^{(\mathrm{D})}} - 1, \forall n, \quad (7c)$$

$$P_{\mathrm{EH},n}(\mathbf{w}_n, \rho_n, \boldsymbol{\Theta}, \mathbf{z}) \ge \mathcal{F}_n(P_{\mathrm{DC},n}^{(\mathrm{D})}), \forall n, \quad (7d)$$

$$P_{\mathrm{EH},l}(\mathbf{w}_n, \boldsymbol{\Theta}, \mathbf{z}) \ge \mathcal{F}_l(P_{\mathrm{DC},l}^{(\mathrm{D})}), \forall l, \quad (7e)$$

$$\gamma_{l,n}(\mathbf{w}_n, \boldsymbol{\Theta}, \mathbf{z}) \le 2^{R_l^{(\mathrm{E})}} - 1, \forall l, n, \quad (7f)$$

$$0 < \rho_n < 1, \forall n, \quad (7g)$$

$$|\boldsymbol{\Theta}_{[q,q]}| \le 1, \forall q. \quad (7h)$$

(7a) represents the energy-efficiency indicator, where R_n is the rate of the n^{th} dual-demand users of the network. Among them, P_{total} is given as

$$P_{\mathrm{total}} = P_T + P_B + \epsilon\left(\sum_{n=1}^{N_D} R_n\right), \quad (8)$$

where P_T is the transmitting power related to the beamforming and P_B is the static consumption of circuits. Moreover, ϵ denotes the power usage per unit data rate. Furthermore, the according power budget is shown as (7b), where P_{Max} is the maximum transmitting power. (7d) and (7e) are the power demand for two types of users, where $\mathcal{F}$ denote the non-linear power conversion equation in [11]. (7c) is the legal SINR requirement and (7f) is the secure transmission demand for the network. (7g) is the limitation of power splitting. (7h) is the physical restriction for RIS.

III. Optimization Approach

There are several variables for the problem and they are coupled with each other. For effectively solving the problem $\mathbf{P}_0$,alternative-resolving approaches are introduced. After separating, there will be two main subproblems. The one refers to

the beamforming vectors, artificial noise, and power-splitting ratio. The other one is related to the optimization of the RIS.

A. The solution for the first subproblem

Although we do not consider the reflection coefficients of the RIS temporarily, the subproblem still is very intractable. First, we will transfer the beamforming vectors and artificial noise into a more manageable form with a semi-definite relaxation scheme. Particularly, the variables can be rewritten as

$$\mathbf{Z}=\mathbf{z}\mathbf{z}^H, \mathbf{W}_n=\mathbf{w}_n\mathbf{w}_n^H, \tag{9}$$

Specifically, (9) has to introduce the extra constraints $\mathbf{Z}\succeq\mathbf{0}$, $\text{rank}(\mathbf{Z})=1$, $\mathbf{W}_n\succeq\mathbf{0}$, and $\text{rank}(\mathbf{W}_n)=1$. Nevertheless, the power-related item of $\mathbf{P}_0$ can be presented in the trace form as

$$|\mathbf{h}_n\mathbf{w}_n|^2=\text{Tr}\left(\mathbf{H}_n\mathbf{W}_n\right), \tag{10}$$

Indeed, the trace form is closer to the requirements of convex programming. Nevertheless, the subproblem still remains some tough items. In detail, the fractional expression of the energy-efficiency indicator (7a) should be transformed further. With the introduced slack variable g_n, we can achieve its subtractive expression.

$$\Omega=\sum_{n=1}^{N_D}g_n-\xi^*\left(P_T+P_B+\epsilon\left(\sum_{n=1}^{N_D}g_n\right)\right). \tag{11}$$

It needs to explain that this transformation can be met only under ξ^* is unique zero. Moreover, ξ^* should be updated during the optimization. This whole process refers to the famous DinkleBach's algorithm.

Due to the adopted variable g_n, we need to add three more constraints related to SINR in (4) as

$$\text{Tr}\left(\mathbf{H}_n\mathbf{W}_n\right)\geq\exp(u_n+v_n),\forall n, \tag{12}$$

$$\exp(u_n)\geq 2^{(g_n)}-1,\forall n, \tag{13}$$

$$\text{Tr}\left(\mathbf{H}_n\left(\sum_{k\neq n}^{N_D}\mathbf{W}_k+\mathbf{Z}\right)\right)+\sigma_1^2+\frac{\delta_2^2}{\rho_n}\leq\exp(v_n),\forall n, \tag{14}$$

where u_n and v_n are the introduced variables. Nevertheless, for tackling them, the SCA scheme should be deployed. Then the problem $\mathbf{P}_0$ can be rewritten as

$$\mathbf{P}_1:\quad\max\Omega \tag{15}$$

$$\text{s.t.}\quad\exp(\dot{u}_n)+\exp(\dot{u}_n)(\dot{u}_n-u_n)\geq 2^{(g_n)}-1,\forall n, \tag{16}$$

$$\text{Tr}\left(\mathbf{H}_n\left(\sum_{k\neq n}^{N_D}\mathbf{W}_k+\mathbf{Z}\right)\right)+\sigma_1^2+\frac{\delta_2^2}{\rho_n}\leq\exp(\dot{v}_n)+\exp(\dot{v}_n)(\dot{v}_n-v_n),\forall n, \tag{17}$$

$$\mathbf{Z},\mathbf{W}_n\succeq\mathbf{0},\forall n,$$

(7c)-(7g), (12)

Algorithm 1. The solution approach for SCA scheme.

INPUT: $\varepsilon_{\text{DK}},\varepsilon_{\text{SCA}}$

While $D_{\text{DK}}\geq\varepsilon_{\text{DK}}$

  While $D_{\text{SCA}}\geq\varepsilon_{\text{SCA}}$

    Solve the problem $\mathbf{P}_1$ to get the optimized variables;

    Update feasible values in (12), (15)-(17) of SCA;

    Achieve D_{SCA} with the values of the different iterations;

  End While

  Update the value of ξ^*.

  Achieve D_{SCA} with the values of the different iterations.

End While

Achieve the beamforming vectors and artificial noise with Gaussian randomization and eigen transformation.

OUTPUT: The optimal vectors.

where $\dot{v}_n$ and $\dot{u}_n$ are the feasible points of u_n and v_n. The whole solving approach can be found in algorithm 1 by dropping the rank one constraint.

B. The solution for the second subproblem

As for the second subproblem of the RIS, the double-inversion model (1) renders the problem more tough. We employ the Sherman-Morrison transformation to simplify it. First, (1) can be written in its equivalent form (18).

$$\mathbf{h}_n(\hat{\theta}_j)=\mathbf{s}_{RT,n}+\mathbf{s}_{RI,n}(-\mathbf{S}_{II}+\mathbf{Q}_j+\hat{\theta}_j\mathbf{g}_j\mathbf{g}_j^T)^{-1}\mathbf{S}_{IT,n}, \tag{18}$$

where the according parameter can be achieved as $\hat{\theta}_j=\mathbf{\Theta}^{-1}_{[j,j]}$ and $\mathbf{Q}_j$ is the matrix $\mathbf{\Theta}^{-1}$ with the $\mathbf{\Theta}^{-1}_{[j,j]}=0$. Moreover, $\mathbf{g}_j$ is the $N_I\times 1$ vector with all zero elements except that the j^{th} element is one. When $\mathbf{Q}_j$ is given, the variable is only $\hat{\theta}_j$, which means the form is more tractable. Then when we adopt the Sherman-Morrison formula, the equivalent expression is given for (18).

$$(-\mathbf{S}_{II}+\mathbf{Q}_j+\hat{\theta}_j\mathbf{g}_j\mathbf{g}_j^T)^{-1}=\left(\left(-\mathbf{S}_{II}+\mathbf{Q}_j\right)^{-1}-\frac{\left(-\mathbf{S}_{II}+\mathbf{Q}_j\right)^{-1}\mathbf{g}_j\mathbf{g}_j^T\left(-\mathbf{S}_{II}+\mathbf{Q}_j\right)^{-1}}{\frac{1}{\hat{\theta}_j}+\mathbf{g}_j^T\left(-\mathbf{S}_{II}+\mathbf{Q}_j\right)^{-1}\mathbf{g}_j}\right), \tag{19}$$

With (19), the model (18) can be reformed as

$$\mathbf{h}_n(c_j) = \mathbf{f}_{n,j} + \frac{1}{c_j}\mathbf{m}_{n,j}, \tag{20}$$

where the notations can be presented with the parameters in (18).

$$c_j = \frac{1}{\hat{\theta}_j} + \mathbf{g}_j^T\left(-\mathbf{S}_{II} + \mathbf{Q}_j\right)^{-1}\mathbf{g}_j, \tag{21}$$

$$\mathbf{f}_{n,j} = \mathbf{s}_{RT,n} + \mathbf{s}_{RI,n}(-\mathbf{S}_{II} + \mathbf{Q}_j)^{-1}\mathbf{S}_{IT,n}, \tag{22}$$

$$\begin{aligned}\mathbf{m}_{n,j} = -\mathbf{s}_{RI,n}((-\mathbf{S}_{II} + \mathbf{Q}_j)^{-1}\mathbf{g}_j \\ \times\mathbf{g}_j^T(-\mathbf{S}_{II} + \mathbf{Q}_j)^{-1})\mathbf{S}_{IT,n}.\end{aligned} \tag{23}$$

So far, the model (20) has a similar form to the normal cascaded channel model, which can be applied by the SDR again. (18) can be reformed by $\mathbf{h}_n(\hat{\mathbf{c}}_j) = \hat{\mathbf{c}}_j\mathbf{e}_{n,j}$, where $\hat{\mathbf{c}}_j = [\frac{1}{c_j}, 1]$ and $\mathbf{e}_{n,j} = [\mathbf{m}_{n,j}; \mathbf{f}_{n,j}]$. Particularly, the notations $\hat{\mathbf{C}}_j = \hat{\mathbf{c}}_j^H\hat{\mathbf{c}}_j$ and the constraints $\hat{\mathbf{C}}_j \succeq 0$ and $\mathrm{rank}(\hat{\mathbf{C}}_j) = 1$ is introduced. Then $\hat{\mathbf{c}}_j$ will be updated one by one until the stop condition is satisfied. The exhausted algorithm framework is not shown here due to the similar algorithm 1.

IV. Simulations Results

A. Harware Design

The S-parameters encapsulate the hardware characteristics of RIS and are crucial for understanding its impact on the network. To begin assessing this influence, we must extract these parameters. In our case, we're working with an 8-element linear array RIS, simulated using HFSS, an electromagnetic analysis software. This RIS setup features 8 elements arranged in a patch configuration, a commonly used design in RIS applications. Each patch primarily consists of a rectangular radiation component and a transmission line as in Fig. 2. To enable control, the termination of the transmission line can be connected to components like a varactor. Moreover, the distance between the elements d_r are configured to simulate the various effects brought from the RIS.

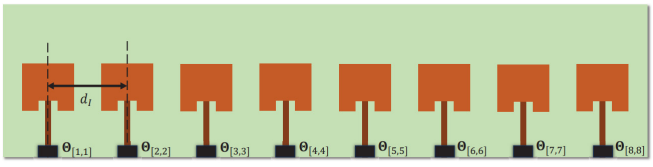

Figure 2. The desgin of the RIS array.

With the extracted $\mathbf{S}_{II}$, the simulations can be conducted. Then other parameter settings are $R_n^{(\mathrm{D})} = 3\mathrm{bit/s/Hz}, \forall n$, $R_l^{(\mathrm{E})} = 1\mathrm{bits/s/Hz}, \forall l$, $P_{\mathrm{DC}}^{(\mathrm{D})} = 1.3\mu\mathrm{W}$, $\sigma_1^2 = -50\mathrm{dBm}$, $\delta_2^2 = -70\mathrm{dBm}$.

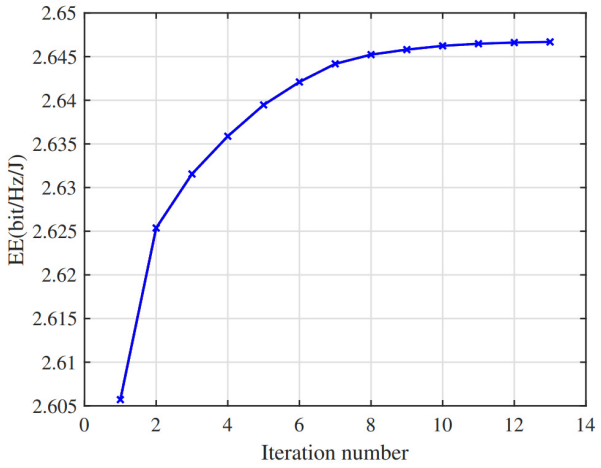

Figure 3. The convergence behavior of the algorithm 1.

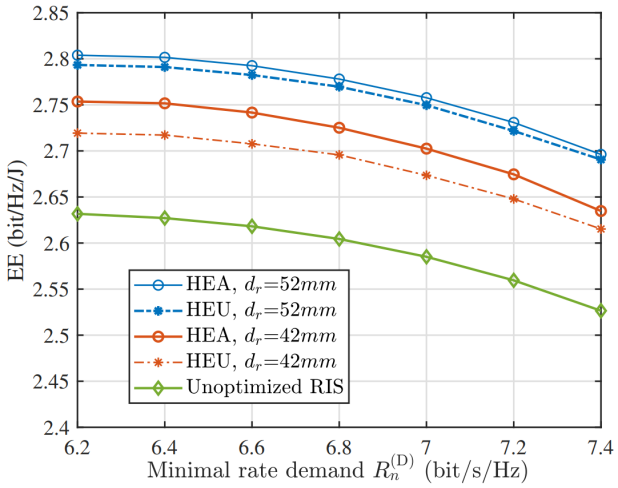

Figure 4. The effect of rate demand on energy efficiency.

B. Parameter settings

Concerning algorithm 1, we show its convergence behavior as in Fig. 3. After several iterations, the energy-efficiency indicators smoothly converge to stable values.

Then the impacts of rate demand $R_n^{(\mathrm{D})}$ on energy-efficiency indicators are shown in this part. An in-depth analysis of hardware effects (HE), encompassing matching and mutual coupling (MC) effects, is conducted. Fig. 4 illustrates the outcomes of HE awareness (HEA), which are optimized considering these effects, while HE unawareness (HEU) denotes optimized variables based on ideal scenarios. Notably, performance gaps are more pronounced in compact RIS configurations due to significant mismatching and strong MC effects. Additionally, HEA and HEU results in $d_r = 52mm$ outperform those in $d_r = 42mm$ owing to larger physical space.

These findings underscore the need for careful trade-offs between network performance and RIS configurations. Despite

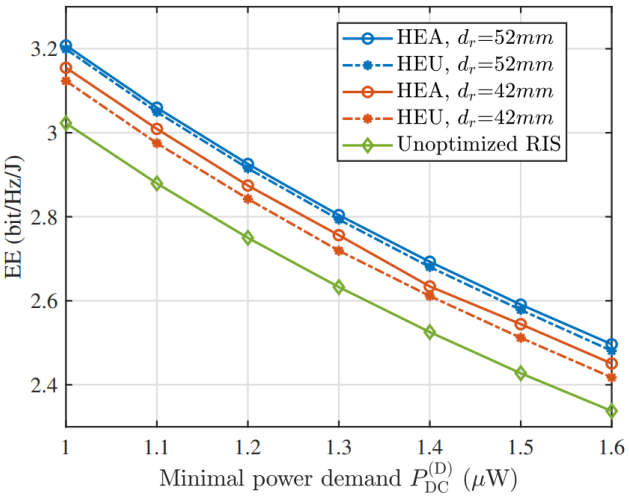

Figure 5. The effect of power requirement on energy efficiency.

differing energy efficiency levels, all cases outperform unoptimized RIS situations, highlighting the pivotal role of RIS in SWIPT networks.

The power requirement, closely tied to network power dissipation, significantly influences energy-efficiency performance, as depicted in Fig. 5. Comparative cases align with those in Figure Fig. 4, with HEA consistently exhibiting superior EE performance. Similar to previous part, detailed explanations are omitted here due to analogous reasons. Across all cases, declining EE trends stem from continuous power resource input to meet increasing requirements. This underscores the importance of low-power receiver design for achieving high EE targets.

V. Conclusion

In this paper, for encompassing crucial physical features of all end devices, we employ an S-parameter-based analysis approach to construct an end-to-end model. Then an EE maximization problem, constrained by QoS requirements and physical limitations, is formulated. Notably, security concerns are addressed by restricting unauthorized rates of the energy-harvesting receive. For resolving the issue, we adopt an alternative strategy to separate coupled variables. Furthermore, the optimization of load reflection coefficients of RIS is achieved through a novel one-by-one optimization scheme leveraging the Sherman-Morrison formula. This strategy, tailored to practical scenarios, integrates RIS hardware characteristics effectively. Simulation results affirm the efficiency of the proposed model and algorithms. Additionally, it is emphasized that hardware characteristics, particularly in compact RIS-augmented networks, are crucial. Future endeavors aim to extend the end-to-end model by incorporating more physical hardware components to better mirror real communication systems.

References

[1] W. Shi, W. Xu, X. You, C. Zhao and K. Wei, "Intelligent Reflection Enabling Technologies for Integrated and Green Internet-of-Everything Beyond 5G: Communication, Sensing, and Security," in IEEE Wireless Communications, vol. 30, no. 2, pp. 147-154, 2023.

[2] R. Deng, J. Chen, C. Yuen, P. Cheng and Y. Sun, "Energy-Efficient Cooperative Spectrum Sensing by Optimal Scheduling in Sensor-Aided Cognitive Radio Networks," in IEEE Transactions on Vehicular Technology, vol. 61, no. 2, pp. 716-725, 2012.

[3] W. Lu et al., "OFDM based bidirectional multi-relay SWIPT strategy for 6G IoT networks," in China Communications, vol. 17, no. 12, pp. 80-91, 2020.

[4] C. Pan et al., "Intelligent Reflecting Surface Aided MIMO Broadcasting for Simultaneous Wireless Information and Power Transfer," in IEEE Journal on Selected Areas in Communications, vol. 38, no. 8, pp. 1719-1734, 2020.

[5] X. Xia, D. Wang, J. Zhao, Z. Zhang and X. You, "Joint Energy Harvesting and Transmission Optimization for Cell-Free Massive MIMO With Network-Assisted Full Duplexing," in IEEE Transactions on Vehicular Technology, vol. 72, no. 6, pp. 7439-7453, 2023.

[6] Z. Chen, J. Tang, X. Y. Zhang, Q. Wu, G. Chen and K. -K. Wong, "Robust Hybrid Beamforming Design for Multi-RIS Assisted MIMO System With Imperfect CSI," in IEEE Transactions on Wireless Communications, vol. 22, no. 6, pp. 3913-3926, 2023.

[7] K. Wang, Q. Zhang and Q. Zhang, "Electromagnetic Simulation of 2.5-Dimensional Cylindrical Metasurfaces With Arbitrary Shapes Using GSTC-MFCM," in IEEE Access, vol. 8, pp. 142101-142110, 2020.

[8] R. Fara, P. Ratajczak, D. -T. Phan-Huy, A. Ourir, M. Di Renzo and J. de Rosny, "A Prototype of Reconfigurable Intelligent Surface with Continuous Control of the Reflection Phase," in IEEE Wireless Communications, vol. 29, no. 1, pp. 70-77, 2022.

[9] X. Yu, J. Xu, N. Zhao, X. Wang and D. Niyato, "Secure Integrated Sensing and Communication Aided by IRS-UAV," GLOBECOM 2023 - 2023 IEEE Global Communications Conference, Kuala Lumpur, Malaysia, 2023, pp. 1735-1740.

[10] Y. Li, H. Zhang, K. Long and A. Nallanathan, "Exploring Sum Rate Maximization in UAV-Based Multi-IRS Networks: IRS Association, UAV Altitude, and Phase Shift Design," in IEEE Transactions on Communications, vol. 70, no. 11, pp. 7764-7774, 2022.

[11] W. Jaafar, L. Bariah, S. Muhaidat and H. Yanikomeroglu, "Time-Switching and Phase-Shifting Control for RIS-Assisted SWIPT Communications," in IEEE Wireless Communications Letters, vol. 11, no. 8, pp. 1728-1732, 2022.

[12] A. Abrardo, D. Dardari, M. Di Renzo and X. Qian, "MIMO Interference Channels Assisted by Reconfigurable Intelligent Surfaces: Mutual Coupling Aware Sum-Rate Optimization Based on a Mutual Impedance Channel Model," in IEEE Wireless Communications Letters, vol. 10, no. 12, pp. 2624-2628, 2021.

[13] H. Li, W. Cai, Y. Liu, M. Li, Q. Liu and Q. Wu, "Intelligent Reflecting Surface Enhanced Wideband MIMO-OFDM Communications: From Practical Model to Reflection Optimization," in IEEE Transactions on Communications, vol. 69, no. 7, pp. 4807-4820, 2021.

[14] M. Najafi, V. Jamali, R. Schober and H. V. Poor, "Physics-Based Modeling and Scalable Optimization of Large Intelligent Reflecting Surfaces," in IEEE Transactions on Communications, vol. 69, no. 4, pp. 2673-2691, 2021.

[15] S. Shen, B. Clerckx and R. Murch, "Modeling and Architecture Design of Reconfigurable Intelligent Surfaces Using Scattering Parameter Network Analysis," in IEEE Transactions on Wireless Communications, vol. 21, no. 2, pp. 1229-1243, 2021.

[16] R. Ma, J. Tang, X. Y. Zhang, K. -K. Wong and J. A. Chambers, "RIS-Assisted SWIPT Network for Internet of Everything Under the Electromagnetics-Based Communication Model," in IEEE Internet of Things Journal (early access).